

Simple solutions of fireball hydrodynamics for rotating and expanding triaxial ellipsoids and final state observables

M. I. Nagy^{1,2} and T. Csörgő^{3,4}

¹*ELTE, H-1118 Budapest XI, Pázmány P. 1/A, Hungary*

²*Departments of Chemistry and Physics, Stony Brook University, Stony Brook, New York 11794, USA*

³*MTA WIGNER FK, H-1525 Budapest 114, POB 49, Hungary and*

⁴*KRF, H-3200 Gyöngyös, Mátrai út 36, Hungary*

We present a class of analytic solutions of non-relativistic fireball hydrodynamics for a fairly general class of equation of state. The presented solution describes the expansion of a triaxial ellipsoid that rotates around one of the principal axes. We calculate the hadronic final state observables such as single-particle spectra, directed, elliptic and third flows, as well as HBT correlations and corresponding radius parameters, utilizing simple analytic formulas. We call attention to the fact that the final tilt angle of the fireball, an important observable quantity, is not independent on the exact definition of it: one gets different angles from the single-particle spectra and from HBT measurements. Taken together, it is pointed out that these observables may be sufficient for the determination of the magnitude of the rotation of the fireball. We argue that observing this rotation and its dependence on collision energy would reveal the softness of the equation of state. Thus determining the rotation may be a powerful tool for the experimental search for the critical point in the phase diagram of strongly interacting matter.

PACS numbers: 24.10.Nz, 47.15.K

I. INTRODUCTION

The quest for the experimental investigation of hot and dense strongly interacting matter has always had a fruitful connection to hydrodynamics. The development of hydrodynamical models that incorporate more and more details about the expansion dynamics of the matter produced in nucleus-nucleus collisions has been going together hand-in-hand with the richer and richer experimental observations on the particle production mechanism. From the early days of statistical modelling of multiplicity distributions in high-energy collisions (pioneered by Fermi) through the hydrodynamical description of rapidity distributions (by the famous Landau-Khalatnikov solution [1–3] as well as the Hwa-Bjorken solution [4, 5]) nowadays we have various exact analytic as well as numerical solutions of hydrodynamics at hand, that strive to describe refined observations on essentially three-dimensional momentum spectra (rapidity as well as transverse mass distributions along with various order azimuthal anisotropy parameters), two-particle Bose-Einstein (also named HBT) correlations with resolving power on dependence on average momentum, azimuthal angle, and many other observables. It is impossible to review all these developments here; for a brief summary of hydrodynamical modeling, see e.g. Ref. [6] and references therein.

A relatively recent research direction in heavy-ion physics phenomenology is the effort to take the rotation of the created strongly interacting matter into account. In non-central heavy-ion collisions, the non-zero initial

angular momentum of the matter influences the time development, and numerical modellings of this rotation (of which now there are many, some pioneering work is to be found in Refs. [7–9]) predict effects on several observables. According to these models, the effect of rotation can generally be thought of as that of an effective radial flow [10] that influences the spectra, the elliptic flow as well as two-particle HBT correlations. An equally important prediction was that, assuming local thermal equilibrium for spin degrees of freedom [11], baryons will be produced with non-zero polarization from a rotating system [12, 13]. To observe this, Λ baryons are promising candidates, since their polarization can be measured with current experimental setup, by studying their decay kinematics.

On another notice, it was known for long that particle production from a source whose shape is ellipsoid-like results in a characteristic oscillation of the HBT radius parameters as a function of pair azimuthal angle, and if the ellipsoid is tilted in coordinate space by a fixed angle, it also results in the appearance of cross-terms in the Gaussian approximation of the correlation function. A simple model with these features can be read in Ref. [14], and a more thorough and fully hydrodynamically inspired derivation of this feature is given in Ref. [15]. Refs. [8, 9] also proposed the differential HBT method to infer the angular momentum of the fireball. However, it was also pointed out that it is hard to disentangle the effects of rotation on the HBT radii.

Nowadays one of the most interesting questions in heavy-ion physics concerns the existence (and if it ex-

ists, the location) of a critical endpoint on the phase diagram of strongly interacting matter, as well as the precise experimental determination of the location of the quark-hadron transition on this phase diagram. Already some investigations based on the finite-size scaling properties of measured system sizes and freeze-out time duration in heavy-ion collisions suggest that a critical endpoint is in reach with current beam energies at the RHIC accelerator [16, 17]. However, as of now, much additional work is needed to underpin this statement and to explore better the phenomenological properties of this transition. One of the paths to achieve this is to systematically investigate the equation of state of the produced matter as a function of beam energy.

The determination of the rotation of the system can give a very useful input to achieve this goal. The importance of rotation — besides the fact that as an effect that influences final state observables, it is interesting on its own — is that the time development of angular velocity of an expanding system depends on how violent is the expansion, which in turn depends on the equation of state (EoS) of the matter. The main reasons behind this are easy to grasp. On one hand, if the initial energy density is fixed, then a softer EoS results in less rapid increase of the moment of inertia (because of lower pressure), which leads to higher angular velocity as compared to stiffer EoS. Another important effect is that adiabatic expansion of a substance with stiffer EoS means more rapid decrease of the temperature with a given volume change, so for similar time-evolution of the volume of the system, a softer EoS means slower decrease of the temperature, meaning that there is more time for the system to rotate before reaching the freeze-out temperature, where the final state observables take their values. In the following (see Section V, we will demonstrate these two effects, and how their interplay influence the final rotation angle of the expanding system.

Rotation is also noteworthy because if one wants to investigate experimentally the EoS of the matter using hadronic final state observables, it is important to have knowledge also on the initial conditions of the flow, since different initial conditions and equations of state can lead to similar final states, making the final state taken alone incapable of determining the EoS. The initial rotational angle of the system can be thought of as either zero or at least as a monotonic function of the energy of the colliding heavy ions, while the EoS — and thus the final rotation angle — is not necessarily monotonic: when searching the critical point via the softening of the EoS, it is precisely such a non-monotonic behavior that one is looking for.

The vast work in the field of numerical hydrodynamics and models based on analytic solutions of hydrodynamics supplement each other well. Analytic models that strive to use exact solutions of both relativistic and non-relativistic hydrodynamics for the description of particle production are naturally harder to find and more specialized in their initial conditions, but once found, they give

general insights in the mechanisms involved in the origin of observables. Recent developments concerning exact relativistic and non-relativistic hydrodynamical solutions with rotation (found both in the framework of AdS/CFT correspondence [18, 19], where the authors also present solutions for non-vanishing shear stress, as well as solutions found by the simultaneous solution of collisionless Maxwell-Boltzmann equation [20]) give much thrust to the effort to better understand the rotational expansion and to disentangle its effects.

In this paper we present a rotating solution of the non-relativistic hydrodynamical equations that is well suited to the geometrical picture of the strongly interacting matter created in heavy ion collisions. The presented solution features ellipsoidal level surfaces of temperature as well as density, with three different principal axes. It is a natural generalization of our earlier results presented in Refs. [21, 22], where we explored exact analytic non-relativistic rotating spheroidal solutions of hydrodynamics, as well as the effect of rotation on the observables. In the solutions discussed in these previous works, the level surfaces of density as well as temperature are spheroids (i.e. ellipsoids with the two principal axes perpendicular to the rotation axis being equal). Also, our new solution fits into a long line of self-similar but not rotating solutions of hydrodynamics, both relativistic and non-relativistic ones [15, 23–29]; these solutions, and the so-called Buda-Lund hydrodynamical parametrization [30, 31] that gives a reasonable relativistic extension of them, have proven to be adequate tools in the description of hadronic observables.

The structure of this paper is as follows. In Section II we recite the hydrodynamical equations suited for the treatment of our problem at hand. It turns out that the solution that we are after can be easily written up in a rotating reference frame instead of the laboratory frame of the colliding nuclei. In Section III we present the solution for an expanding rotating triaxial ellipsoid (i.e. an ellipsoid with three different axes), and with a self-similar velocity and density field. The presented solution generalizes our previous results on rotating spheroidal [21] as well as non-rotating ellipsoidal [15, 26] solutions. In Section IV we calculate the final state hadronic observables (spectra, flow parameters, HBT correlation function) using simple analytical formulas. These formulas enable us to draw some general conclusions on the effect of rotation on the observables. In Section V we illustrate the time development of the system as well as the effect of rotation on the observables using some simple and reasonable initial conditions. The detailed investigation of the available experimental data is beyond the scope of this paper, however, we point out that the simultaneous measurement of the harmonic flow parameters (v_1 , v_2 , v_3) and the azimuthal oscillation of HBT radii (especially the cross-terms in the so-called Bertsch-Pratt parametrization) gives a means to determine the angular velocity as well as the final tilt angle of the ellipsoidal expanding system, providing a path to determine the softness of the

equation of state as outlined above. Finally we summarize and conclude.

II. BASIC EQUATIONS

A. Equations of hydrodynamics

We outline the non-relativistic hydrodynamical equations in a form suited to our task of finding rotating exact solutions. The fluid motion is described by the velocity field \mathbf{v} , the pressure p , the energy density ε , the temperature T , the particle number density n , the chemical potential μ , and the entropy density σ . All these hydrodynamical quantities are functions of t and \mathbf{r} , the time and the spatial coordinate. The fundamental equations are the particle number and energy conservation equations as well as the Euler equation:

$$\partial_t n + \nabla(n\mathbf{v}) = 0, \quad (1)$$

$$\partial_t \varepsilon + \nabla(\varepsilon\mathbf{v}) = -p(\nabla\mathbf{v}). \quad (2)$$

$$\partial_t \mathbf{v} + (\mathbf{v}\nabla)\mathbf{v} = -\nabla p/(m_0 n). \quad (3)$$

Here m_0 is the mass of an individual particle. Using the well-known thermodynamical relations

$$\varepsilon + p = T\sigma + \mu n, \quad (4)$$

$$d\varepsilon = Td\sigma + \mu dn, \quad (5)$$

one can verify that the energy conservation equation Eq. (2) is equivalent to the entropy conservation:

$$\partial_t \sigma + \nabla(\sigma\mathbf{v}) = 0. \quad (6)$$

This set of equations need to be supplemented by an appropriate equation of state providing a relation between T , p and ε . As in Refs. [15, 21], here we also investigate the following EoS:

$$p = nT, \quad (7)$$

$$\varepsilon = \kappa(T)p. \quad (8)$$

This EoS is thermodynamically consistent for any $\kappa(T)$ function, as was shown (using the free energy density as a thermodynamical potential) e.g. in Ref. [15]. This EoS is a generalization of the case for constant κ , which would correspond to a non-relativistic ideal gas for $\kappa = 3/2$, and to an ultra-relativistic ideal gas for $\kappa = 3$. The arbitrary $\kappa(T)$ function introduced here allows one to incorporate any temperature dependent speed of sound, which is usually introduced as $c_s^2 = dp/d\varepsilon = 1/\kappa(T)$.

Just as in Ref. [21], we may rewrite Eqs. (1)–(3) for the independent variables T , n and \mathbf{v} as follows:

$$(\partial_t + \mathbf{v}\nabla)n = -n\nabla\mathbf{v}, \quad (9)$$

$$\left[T \frac{d\kappa}{dT} + \kappa\right](\partial_t + \mathbf{v}\nabla)T = -T\nabla\mathbf{v}, \quad (10)$$

$$nm_0(\partial_t + \mathbf{v}\nabla)\mathbf{v} = -n\nabla T - T\nabla n. \quad (11)$$

Also, following Refs. [21, 22], we note here that this set of equations is valid for the case when there is non-vanishing

n particle density which embodies the fact that there is a meaningful total particle number that is conserved. This assumption is valid for the late stages of the hydrodynamic evolution of the matter produced in heavy-ion collisions, when the kinetic freeze-out is not yet reached but the particle type changing hadronic reactions ceased to play a role. For the case generally thought to apply to the quark-gluon-plasma phase, that is, when there is no conserved particle density, we may (again following Ref. [21]) write up a separate set of hydrodynamic equations, the main difference being that here the only independent variables are T , σ and \mathbf{v} , and the mass term in the Euler equation is different:

$$\partial_t \sigma + \nabla(\sigma\mathbf{v}) = 0, \quad (12)$$

$$(\varepsilon + p)(\partial_t \mathbf{v} + (\mathbf{v}\nabla)\mathbf{v}) = -\nabla p, \quad (13)$$

which, using the thermodynamical relation $dp = \sigma dT$ (which is valid for $n = 0$) is rewritten as

$$(\partial_t + \mathbf{v}\nabla)\sigma = -\sigma\nabla\mathbf{v}, \quad (14)$$

$$T(\partial_t + \mathbf{v}\nabla)\mathbf{v} = -\nabla T. \quad (15)$$

The mass term $\varepsilon + p$ in the Euler equation (the enthalpy density) stems from the relativistic version of the Euler equation. In case when there is a conserved particle number, one is led to make the approximation $\mu \approx m_0$, and thus $\varepsilon + p = T\sigma + \mu n \approx m_0 n$. The case for vanishing n is seen somehow as the opposite limiting case, when the mass term is solely stemming from the entropy density.

The basic equations for vanishing n , Eqs. (14) and (15) also have to be supplemented with an EoS. The convenient choice again is simply

$$\varepsilon = \kappa(T)p \Leftrightarrow [\kappa(T) + 1]p = T\sigma. \quad (16)$$

With an appropriate $\kappa(T)$ function, one can describe e.g. the equation of state of the strongly interacting matter inferred from lattice QCD calculations.

As seen already in Ref. [21], the solution of these two sets of equations (one valid for non-vanishing n , the other for vanishing n) can be done very similarly to each other; this is also true for the solutions presented in this paper. In the following, we mainly restrict ourselves to the case when there is a conserved n , i.e. to the solution of Eqs. (1)–(3), mainly because we want to calculate the final state hadronic observables which are formed in the final states of the hydrodynamical evolution, where this approximation is thought to be valid.

B. Equations in a rotating reference frame

For our treatment, the shape of the hot and dense matter that is created in non-central heavy-ion collisions can be now approximated with a triaxial ellipsoidal shape that has non-zero angular momentum, and also expands violently. As customary in heavy-ion phenomenology, let the z axis point in the direction of the incoming projectiles, and the x axis point in the direction of the impact

parameter. In this way, the rotation is assumed to be in the x - z plane, around the y axis. In the following this frame is called the laboratory frame, denoted by K .

It turns out that finding a solution which describes the physical situation of interest to us, i.e. a triaxial, expanding and simultaneously rotating ellipsoid, is simpler to achieve in a frame which rotates together with the expanding ellipsoid. This frame is denoted by K' , with its axes, x' , y' and z' , pointing in the directions of the principal axes. The y' axis is the same as the y axis. We denote the rotation angle of K' with respect to K in the x - z plane by $\vartheta(t)$. (We will sometimes omit the explicit notation of the time dependence for functions introduced as functions of t .) The relation between the components of the coordinate vector in the K and K' frames is

$$r'_x = r_x \cos \vartheta - r_z \sin \vartheta, \quad (17)$$

$$r'_z = r_x \sin \vartheta + r_z \cos \vartheta, \quad (18)$$

or, written in a matrix-vector form,

$$\mathbf{r}' = \mathbf{M}(t)\mathbf{r}, \quad \mathbf{M}(t) \equiv \begin{pmatrix} \cos \vartheta & 0 & -\sin \vartheta \\ 0 & 1 & 0 \\ \sin \vartheta & 0 & \cos \vartheta \end{pmatrix}. \quad (19)$$

The transformation between the two frames, K and K' are thus described by the rotation matrix \mathbf{M} .

We refer to the angular velocity of K' with respect to K as the vector $\boldsymbol{\Omega}$. The relation between the velocity field components in K and K' contains the effect of this angular velocity also:

$$\mathbf{v}' = \mathbf{M}\mathbf{v} - \boldsymbol{\Omega} \times \mathbf{r}', \quad \boldsymbol{\Omega} = \begin{pmatrix} 0 \\ \dot{\vartheta} \\ 0 \end{pmatrix}, \quad (20)$$

or written up in components:

$$v'_x = v_x \cos \vartheta - v_z \sin \vartheta - \dot{\vartheta} r'_z, \quad (21)$$

$$v'_z = v_x \sin \vartheta + v_z \cos \vartheta + \dot{\vartheta} r'_x. \quad (22)$$

The y components do not mix: $v'_y = v_y$, $r'_y = r_y$.

Of Eqs. (1)–(3), the continuity equations retain their form in K' , but the Euler equation needs to be supplemented with inertial force terms in the rotating reference frame. The basic equations in the K' frame are then

$$(\partial'_t + \mathbf{v}' \cdot \nabla') n = -n \nabla' \cdot \mathbf{v}', \quad (23)$$

$$\left[T \frac{d\kappa}{dT} + \kappa \right] (\partial'_t + \mathbf{v}' \cdot \nabla') T = -T \nabla' \cdot \mathbf{v}', \quad (24)$$

$$(\partial'_t + \mathbf{v}' \cdot \nabla') \mathbf{v}' = -\frac{\nabla' T}{m_0} - \frac{T}{n} \frac{\nabla' n}{m_0} + \mathbf{f}', \quad (25)$$

$$\mathbf{f}' \equiv 2\mathbf{v}' \times \boldsymbol{\Omega} + \boldsymbol{\Omega} \times (\mathbf{r}' \times \boldsymbol{\Omega}) + \mathbf{r}' \times \dot{\boldsymbol{\Omega}}. \quad (26)$$

The terms in \mathbf{f}' describe the inertial forces: the Coriolis force, the centrifugal force and the force stemming from the angular acceleration of the K' frame. We introduced the ∇' and ∂'_t notations for the differentiation in

the K' frame: ∇' means derivatives with respect to the \mathbf{r}' coordinates, while ∂'_t denotes time derivative with \mathbf{r}' fixed. This derivative, ∂'_t is different from ∂_t , because the relation between \mathbf{r}' and \mathbf{r} is time-dependent.

In the following Section we present a rotating ellipsoidal solution; we omit some steps of derivation for brevity. All results can be directly checked against Eqs. (23)–(25).

III. ROTATING ELLIPSOIDAL SOLUTIONS

The solution presented is a direct generalization of earlier results describing non-rotating ellipsoidal expansion [15]), as well as rotating solutions (see Refs. [21]). Many features of these earlier results carry over essentially unchanged into our treatment, so in some sense we follow the footsteps outlined in these works, and depart from it at some points to arrive at the desired rotating, triaxial solution. In formulating our new solution, we try to conform our notations to the ones in these earlier works as much as possible.

A. Velocity field and thermodynamical quantities

Following the mentioned earlier works on hydrodynamical solutions with self-similar expanding ellipsoids, we introduce the time-dependent principal axes of the rotating ellipsoid, $X(t)$, $Y(t)$, $Z(t)$, and a *scaling variable* s , whose level surfaces correspond to the ellipsoidal level surfaces of the temperature and density. If we express s in K' , its level surfaces will automatically describe the rotating ellipsoids:

$$s = \frac{r'^2_x}{X^2} + \frac{r'^2_y}{Y^2} + \frac{r'^2_z}{Z^2}. \quad (27)$$

As a generalization of earlier results, we now assume that the velocity field is linear in the coordinates in the rotating frame (this also implies linearity in the K frame, but it turns out that the calculations are easier in the K' frame). We assume also that the flow „preserves” the ellipsoidal $s = \text{const}$ surfaces, i.e. s is a function that remains constant along the trajectories (world-lines) of the fluid elements. This condition can be expressed as

$$(\partial_t + \mathbf{v} \cdot \nabla) s = 0 \quad \Leftrightarrow \quad (\partial'_t + \mathbf{v}' \cdot \nabla') s = 0. \quad (28)$$

It turns out that the most general velocity field satisfying these requirements (linearity and compatibility with the above s) is

$$\mathbf{v}'(\mathbf{r}', t) = \begin{pmatrix} \frac{\dot{X}(t)}{X(t)} r'_x + g(t) \frac{X(t)}{Z(t)} r'_z \\ \frac{\dot{Y}(t)}{Y(t)} r'_y \\ \frac{\dot{Z}(t)}{Z(t)} r'_z - g(t) \frac{Z(t)}{X(t)} r'_x \end{pmatrix}, \quad (29)$$

where $g(t)$ is an up to now arbitrary function of time.

Introducing the characteristic volume $V(t)$ of the expanding ellipsoid, the solution for the continuity equation, Eq. (23) is readily written up as

$$n(\mathbf{r}', t) = n_0 \frac{V_0}{V} \nu(s), \quad V \equiv (2\pi)^{3/2} XYZ, \quad (30)$$

with an arbitrary $\nu(s)$ function. Here V_0 is the value of V at the initial time. The time evolution causes the principal axes X, Y, Z to eventually expand; so do the characteristic ellipsoids (the level surfaces of s), and n decreases. The coordinate dependence enters through s , so the expansion of the density profile is self-similar.

The solution for the temperature equation, Eq. (24) can be found along similar lines as in e.g. Ref. [15]. If the $\kappa(T)$ function is arbitrary, it turns out that only a spatially constant temperature will give a meaningful solution. This $T(t)$ function, as easily seen from Eq. (24), obeys the following differential equation:

$$\left\{ \frac{d}{dT} [T \kappa(T)] \right\} \frac{\dot{T}}{T} + \frac{\dot{V}}{V} = 0, \quad (31)$$

whose solution can be written up implicitly as

$$T \equiv T(t), \quad \ln \frac{V_0}{V} = \int_{T_0}^T dT' \left[\frac{d\kappa(T')}{dT'} + \frac{\kappa(T')}{T'} \right]. \quad (32)$$

In the case of constant κ , we can solve this as

$$\kappa(T) = \kappa = \text{const} \quad \Rightarrow \quad T(t) = T_0 \left(\frac{V_0}{V} \right)^{\frac{1}{\kappa}}. \quad (33)$$

This describes an adiabatic expansion, where the familiar $T^\kappa V = \text{const}$ relation holds.

In case of constant κ , however, just as it was the case in the earlier results (eg. [25, 26]), one can generalize the temperature to be a coordinate-dependent function:

$$T(t) = T_0 \left(\frac{V_0}{V} \right)^{\frac{1}{\kappa}} \mathcal{T}(s). \quad (34)$$

The remaining equation to be solved is the Euler equation, Eq. (25). The expression of the \mathbf{f}' interial force from the definition of \mathbf{v}' , Eq. (29) is straightforward, as is the derivatives of T and n ; one can plug these into Eq. (25). It turns out that there are two conditions that have to be met in order to have a proper solution to the Euler equation: first, the $\nu(s)$ and $\mathcal{T}(s)$ are not independent but obey the condition

$$\nu(s) = \frac{1}{\mathcal{T}(s)} \exp \left(-\frac{1}{2} \int_0^s \frac{ds'}{\mathcal{T}(s')} \right), \quad (35)$$

(just as in Refs. [25, 26]). If the temperature is spatially homogeneous, $T \equiv T(t)$, which is a special case if $\kappa = \text{const}$, but obligatory if $\kappa(T)$ is not constant, the spatial density profile turns out to be Gaussian:

$$T \equiv T(t) = T_0 \left(\frac{V_0}{V} \right)^{\frac{1}{\kappa}} \quad \Leftrightarrow \quad n = n_0 \frac{V}{V_0} e^{-s^2/2}. \quad (36)$$

The second condition for the (25) Euler equation to be solved is that the time dependence of the X, Y, Z principal axes of the rotating ellipsoid as well as that of the up to now arbitrary $\vartheta(t), g(t)$ functions are subject to some ordinary differential equations, the *equations of motion* for these quantities. These equations deserve a thorough investigation, we proceed with this in the following.

B. Equations of motion, integrals

After some calculation one can verify that from the requirement that the (25) Euler equation holds, the only reasonable possibility is that the $g(t)$ and $\vartheta(t)$ are equal, and take the following form:

$$\dot{\vartheta}(t) = g(t) \equiv \frac{\omega(t)}{2}, \quad \omega(t) \equiv \omega_0 \frac{R_0^2}{R^2(t)}, \quad (37)$$

$$R(t) \equiv \frac{X(t) + Z(t)}{2}, \quad R_0 = \frac{X_0 + Z_0}{2}. \quad (38)$$

Here X_0 and Z_0 are the initial values of the X and Z axes (remember, the rotation is around the y axis), and ω_0 is a free parameter. To conform with the earlier spheroidal solutions of Ref. [21], we introduced an „average” angular velocity $\omega(t)$ of the flow, as well as the „average radius” $R(t)$ (and its initial value R_0), this notation will be useful in the following. In the spheroidal limiting case $X = Y = R$, and this R is the same as the radial size of the ellipsoid in the case of the spheroidal solution.

Also we note that of the so-called vorticity of the flow, $\boldsymbol{\omega}(\mathbf{r}, t) \equiv \nabla \times \mathbf{v}(\mathbf{r}, t)$, only the y -component is non-vanishing, and it takes the simple form of

$$\omega_y(\mathbf{r}, t) \equiv (\nabla \times \mathbf{v}(\mathbf{r}, t))_y = 2 \left(\dot{\vartheta} + g \frac{X^2 + Z^2}{2XZ} \right). \quad (39)$$

In the case of $X = Z$, $\omega_y = 2\omega(t)$, just as in Ref. [22]. We will also see that this $\omega(t)$ is the quantity characteristic to the rotation that appears in the expression of the observables in a straightforward way.

To elucidate the characteristic of our velocity field, we note again that our velocity field, taken in the inertial K frame by substituting Eq. (29) into Eqs. (21) and (22), if $X = Z = R$, reduces to the velocity field of Refs. [21]. But it must be noted here that in the case of our new general, $X \neq Z$ solution, it is *not* simply the case that we have a rotating frame K' which is the eigenframe of the rotating ellipsoidal surfaces, and also the velocity field is non-rotating in the K' frame. We see that since the $g(t)$ function in Eq. (29) turned out to be equal to $\dot{\vartheta}$, g and $\dot{\vartheta}$ each „carry” half of $\omega(t)$ — that is, the rotation of the velocity field (in the inertial K frame) has two „components”: first, the ellipsoidal surfaces are rotating (so the K' frame rotates in the K frame, governed by $\dot{\vartheta}(t)$), second, the velocity field rotates with respect to the K' frame (governed by $g(t)$). It turns out after some simple investigation of the Euler equation that one cannot find a solution where $g(t) \equiv 0$ but $\dot{\vartheta}(t) \neq 0$. In Appendix A we get back to this question.

For the principal axes X, Y, Z , one can now write up the equations of motion. In the case when the $\kappa(T)$ function is not constant, and consequently, the solution is valid only if T is spatially homogeneous, as in Eq. (32), the equations of motion are

$$X(\ddot{X} - \omega^2 R) = Y\ddot{Y} = Z(\ddot{Z} - \omega^2 R) = \frac{T}{m_0}, \quad (40)$$

where the time evolution of the temperature T is given by Eq. (32). In case of $\kappa(T) = \kappa = \text{const}$, $T(t)$ has an explicit form as given by Eq. (33). As discussed already, the constant κ case allows a more general, coordinate-dependent temperature, given by Eq. (34). The equations of motion of the axes in this case are similar to Eq. (40), just with the additional prescription that the T in Eq. (40) is to be substituted with the expression of T in the $\mathcal{T}(s) = \text{const}$ case, i.e. with the form given by Eq. (33).

These are ordinary differential equations; although a general analytical solution to them is lacking, in terms of the hydrodynamical problem, they can be considered as readily solvable numerically for any initial conditions $R_0, Y_0, \dot{R}_0, \dot{Y}_0, T_0$ and ω_0 . These equations of motion are natural generalizations of those found in Refs. [15, 21, 22, 26]. It must be remembered, however, that these ones are valid for the axes in the rotating K' frame.

The equations of motion for the principal axes X, Y, Z can be thought of as the equations of motion of a particle with mass m_0 in an external potential. We write up the Hamiltonian governing this motion corresponding to Eq. (40) only in the constant κ case:

$$H = \frac{1}{2m_0}(P_X^2 + P_Y^2 + P_Z^2) + U(X, Y, Z), \quad (41)$$

$$U(X, Y, Z) = \kappa T_0 \left(\frac{V_0}{V} \right)^{1/\kappa} + m_0 \omega^2 R^2. \quad (42)$$

with the definitions of ω and R given by Eqs. (37) and (38). Of course, the momenta P_X, P_Y, P_Z are just equal to $m_0 \dot{X}, m_0 \dot{Y}, m_0 \dot{Z}$, respectively.

In the case of non constant $\kappa(T)$, the Hamiltonian that gives back Eq. (40) also can be written up in a much similar way, the only difference is the form of the temperature related term in the expression of the potential U . We do not indulge in this now, but mention that this can be done in a way similar to that outlined in Ref. [21].

If we set $X = Z \equiv R$ in our equations, we get back the results of Ref. [21]: we see that in this case indeed the ω_0 plays the role of the initial value of the angular velocity of the fluid. Reflecting on the discussion after Eq. (37), it must be noted that in the case of $X = Z$, the meaning of the ϑ angle becomes ill-defined: for a rotating spheroid one clearly cannot uniquely define the tilt of the co-rotating coordinate system *and* the rotational velocity with respect to that frame (determined by the $g(t)$ function) separately. In the spheroidal case only the total angular velocity of the fluid (i.e. that with respect to the inertial K frame) has a definite meaning; as mentioned after Eq. (37), in some sense half of this angular velocity is provided by $\dot{\vartheta}$, the other half by $g(t)$.

C. Conserved quantities

It is also worthwhile to calculate some conserved quantities. We do this only for the case of constant κ , and for simplicity we also specify the spatial shape of the density n and T by taking the spatially homogeneous temperature and Gaussian density case, Eq. (36). In this case, the total particle number N_0 is

$$N_0 = \int d^3 \mathbf{r}' n(t, \mathbf{r}') = n_0 V_0, \quad (43)$$

which is clearly a constant.

The total (kinetic and internal) energy E_0 of the fluid turns out to be

$$E_0 = \frac{m_0}{2} (\dot{X}^2 + \dot{Y}^2 + \dot{Z}^2) + U(X, Y, Z), \quad (44)$$

with $U(X, Y, Z)$ given by Eq. (42). This is precisely the value of the Hamiltonian; the conservation of E_0 is thus equivalent to the Hamiltonian formulation of the equations of motion for X, Y, Z .

Just as in e.g. Ref. [22], in the special case of constant $\kappa(T) = \kappa = 3/2$ (which is the case of a non-relativistic ideal gas), one can write up another first integral of the equations of motion, Eq. (40). Combining these equations with the energy conservation equation obtained from the $H = \text{const}$ criterion, with H defined in Eq. (41), for $\kappa = 3/2$ one gets the following solution for the time evolution of $X^2 + Y^2 + Z^2$:

$$X^2 + Y^2 + Z^2 = \frac{2E_0 t^2}{m_0 N_0} + 2 \left[X_0 \dot{X}_0 + Y_0 \dot{Y}_0 + Z_0 \dot{Z}_0 \right] t + X_0^2 + Y_0^2 + Z_0^2, \quad \text{if } \kappa = 3/2, \quad (45)$$

with the initial conditions taken at $t = 0$. This is a direct generalization of earlier results found in Ref. [38], where a similar result was obtained for triaxial but non-rotating solutions.

Another important quantity is the total angular momentum \mathbf{J}_0 of the fluid. In our setting, only the J_y component is non-zero: its value turns out to be

$$J_y = 2N_0 m_0 \omega_0 R_0^2, \quad R_0 \equiv \frac{X_0 + Z_0}{2}, \quad (46)$$

which is indeed constant. To frame this expression for J_y , we can calculate the (time-dependent) moment of inertia $\Theta(t)$ of the fluid (with respect to the y axis). For the Gaussian shape of n specified by Eq. (36), we get

$$\Theta(t) = m_0 N_0 (X^2 + Z^2) \Rightarrow \quad (47)$$

$$\Rightarrow J_y = \Theta(t) \omega(t) \times \frac{2R^2}{X^2 + Z^2}. \quad (48)$$

We see that the analogy to the spherical case is not complete; our new solution has a richer structure. Also, the rotational motion in our solution is clearly different from

that of a rotating solid body. Nevertheless, again in the $X = Z \equiv R$ special case, the present formulas give back those valid for the spheroidal case.

* * *

In some sense the solution presented above is a fairly general self-similar rotating solution. In Appendix A we outline the reasoning that leads to this solution, and show that from the ansatz specified up to now, a slightly more general solution also may follow. However, for the problem under consideration, namely, the rotating expansion of the fireball produced in heavy-ion collisions, the additional generality in that solution is apparently irrelevant.

It should be also emphasized that (as seen from the treatment of the problem in Appendix A) although one would very much prefer a rotating solution which is a more direct generalization of the previously known ellipsoidal or rotating spherical solutions, i.e. where the ellipsoids co-rotate with the velocity field (in the sense that $g(t) \equiv 0$ in Eq. (29), that is, in the eigenframe of the ellipsoids, K' , the velocity field is non-rotating), such solutions simply do not exist. In this sense the solution presented here is the simplest one corresponding to tri-axial rotating ellipsoids.

IV. CALCULATION OF HADRONIC OBSERVABLES

Having seen a hydrodynamical solution whose time dependence mirrors that of an expanding rotating triaxial ellipsoid, that is a reasonable analytic model for the rotating expanding time evolution of the strongly interacting matter created in heavy-ion collisions, we now turn to the question of what observable quantities carry information on the rotation of the system. It turns out that the hadronic observables for the considered solution can be expressed by means of simple analytic formulas. In this section we outline these calculations and discuss what observables are sensitive to the rotation. We also illustrate the effect of rotation on some observables, for a set of reasonable initial conditions and time evolution.

In the usual way in hydrodynamical modelling, we assume that the system (the fluid) freezes out on some hypersurface, i.e. the hydrodynamical evolution abruptly stops, to give way to the final observable particles. The phase-space distribution of the system at the instant of freeze-out then determines the final state distributions. We specify the solution that we will investigate as well as the freeze-out condition in the simplest way that suits the calculation: we take the spatially homogeneous temperature case (with a Gaussian density profile, Eq. (36)), and assume that the freeze-out sets in at a given T_f temperature. In our $T \equiv T(t)$ case this also means that freeze-out is happening at a given time, t_f , everywhere simultaneously. We assume that at the freeze-out, particles with mass m appear. Throughout the calculation, m is retained as a free parameter, however, in practical cases,

the mass of the produced particles may be taken the fixed values valid for e.g. pions, kaons, or (anti)protons ($m = 140$ MeV, $m = 494$ MeV, and $m = 938$ MeV, respectively). A reasonable assumption for the value of T_f was made already by Landau and Belenkij [2]: $T_f \approx m_\pi$, the pion mass, since this is the typical energy at which the hadronic collisions that transform particle type cease to play a role, and thus this is the typical temperature at which the mean free path of a pion gas starts to increase exponentially.

It may be also noted that our treatment is fully non-relativistic, an assumption that allows a fully analytic calculation, but questionable as a realistic assumption for intermediate transverse momenta. Concerning relativistic parametrizations, an easily performed generalization of the exact formulas stemming from non-relativistic solutions is described in the framework of the so-called Buda-Lund model [30, 31]. The end result here is basically that one may substitute $m_t = \sqrt{p_t^2 + m^2}$ (transverse mass) into the place of the mass m of the individual particles, for a rudimentary relativistic generalization. So the m dependence in our following formulas for the observables may be understood as a preliminary suggestion on the m_t dependence what one might get in a more realistic relativistic treatment. However, in this paper we only deal with fully analytic (thus in our case, non-relativistic) formulas, with m being the mass of the particle.

A. Source function

The observables are calculated from the *source function* or *emission function*, denoted by $S(t, \mathbf{r}, \mathbf{p})$, the thermal phase-space distribution taken at the freeze-out time, t_f . It can be written in our non-relativistic approximation, for our case of solution, as

$$S(\mathbf{r}, \mathbf{p}) \propto \frac{n(t_f, \mathbf{r})}{T_f^{3/2}} \exp \left\{ -\frac{(\mathbf{p} - m\mathbf{v}(t_f, \mathbf{r}))^2}{2mT_f} \right\}, \quad (49)$$

with every hydrodynamical quantity taken at the freeze-out time. This is normalized so that the integral over \mathbf{p} at a given point \mathbf{r} is proportional to the number density, n at that point. Here m stands for the mass of the produced particle which may or may not be equal to the m_0 parameter that governs the time development of the hydrodynamical evolution as in Eq. (40).

One can use this source function to calculate two important set of observables in a hydrodynamical setting: the single particle spectrum (and its corollaries, like azimuthal anisotropies), and two-particle correlation functions (and related quantities, like HBT radii). The defining formula of the single-particle spectrum $N_1(\mathbf{p})$ in our hydrodynamical setting is

$$N_1(\mathbf{p}) \equiv E \frac{dn}{d^3\mathbf{p}} \propto E \int d^3\mathbf{r} S(\mathbf{p}, \mathbf{r}), \quad (50)$$

where E is the particle energy.

Bose-Einstein or HBT-correlations of bosons stem from their quantum mechanical indistinguishability, and in turn, the symmetry property of their wave-function. Assuming interaction-free final state, the two-particle Bose-Einstein correlation function $C(\mathbf{K}, \mathbf{q})$ is connected to the Fourier transform of the emission function:

$$C(\mathbf{K}, \mathbf{q}) \approx 1 + \lambda \frac{|\tilde{S}_{\mathbf{K}}(\mathbf{q})|^2}{|\tilde{S}_{\mathbf{K}}(\mathbf{0})|^2}, \quad (51)$$

with $\mathbf{K} = \frac{1}{2}(\mathbf{p}_1 + \mathbf{p}_2)$ being the average momentum and $\mathbf{q} = \mathbf{p}_1 - \mathbf{p}_2$ the relative momentum of the pair, and

$$\tilde{S}_{\mathbf{K}}(\mathbf{q}) = \int d^3\mathbf{r} e^{i\mathbf{q}\cdot\mathbf{r}} S(\mathbf{r}, \mathbf{K}), \quad (52)$$

with $S(\mathbf{r}, \mathbf{p})$ taken at the average momentum \mathbf{K} . The so-called intercept parameter λ measures the correlation strength at zero momentum. A phenomenological explanation for λ is the so-called core-halo model [33], where it measures the ratio of primordial particles (pions) to all the produced ones (including those which stem from long-lived resonance decays). The approximation in Eq. (51) is, among other things, that one writes \mathbf{K} in the argument of the source function in Eq. (52), and also that one neglects multi-particle correlation effects, correlated particle production, and Coulomb final state interactions (this latter one can be straightforwardly corrected for).

In what follows, we outline the calculations that lead to our results on the observables. The calculations themselves are in essence very simple, since they involve only Gaussian integration, albeit multivariate Gaussians with mixed second-order terms. Using Eqs. (36) and (29), we clearly see that indeed $S(\mathbf{r}, \mathbf{p})$ is Gaussian in the coordinates.

Our hydrodynamical solution outlined in Section III was written up in a rotating reference frame, K' , whose tilt angle with respect to the inertial K frame, $\vartheta(t)$ was one of the dynamical variables of the rotating expansion. We got an expression for $\vartheta(t)$ that can be numerically integrated to yield the final tilt angle $\vartheta_f \equiv \vartheta(t_f)$. The calculation of the observables is most easily done in an *inertial*, i.e. non-rotating reference frame that is tilted with ϑ_f with respect to K . We may denote this frame by \overline{K}' : the momentum components in this frame are related to the K -components similarly as the coordinate \mathbf{r}' to \mathbf{r} :

$$\overline{\mathbf{p}}' = \mathbf{M}\mathbf{p} \quad \Leftrightarrow \quad \begin{aligned} p'_x &= p_x \cos \vartheta - p_z \sin \vartheta, \\ p'_z &= p_x \sin \vartheta + p_z \cos \vartheta, \end{aligned} \quad (53)$$

by using the matrix notation of Eq. (19). However, the velocity field $\overline{\mathbf{v}}'$ in the \overline{K}' frame is different from \mathbf{v}' as introduced in Eq. (20) precisely because the \overline{K}' frame is inertial, so $\overline{\mathbf{v}}'$ does *not* contain the effect of angular motion:

$$\overline{\mathbf{v}}' = \mathbf{M}\mathbf{v} \quad \Leftrightarrow \quad \begin{aligned} \overline{v}'_x &= v'_x + \dot{\vartheta} r'_z, \\ \overline{v}'_z &= v'_z - \dot{\vartheta} r'_x. \end{aligned} \quad (54)$$

The coordinates in the \overline{K}' frame are of course the same as those in K' , with the components of that of \mathbf{r}' . Again, the y components do not mix: $p'_y = p_y$, $\overline{v}'_y = v'_y = v_y$.

We need to plug these expressions into Eq. (49). So the final expression of the source function is

$$S(\mathbf{r}', \mathbf{p}') \propto \frac{n_0}{T_f^3} \exp\left(-\frac{r'^2_x}{2X_f^2} - \frac{r'^2_y}{2Y_f^2} - \frac{r'^2_z}{2Z_f^2}\right) \times \exp\left(-\frac{1}{2mT_f}(\mathbf{p}' - m\overline{\mathbf{v}}'(\mathbf{r}', t_f))^2\right). \quad (55)$$

B. Single particle spectrum

As already mentioned, the calculations leading to the results below are simple Gaussian integrals, as seen from Eq. (55): the particle number density n is of Gaussian form, and the Maxwellian term for a velocity field linear in the coordinates also yields a Gaussian shape. The only complication compared to Refs. [15, 22] is that the desired integrals contain also off-diagonal, $r'_x r'_z$ terms. After some calculation, one arrives at the following expression for $\frac{dn}{d^3\mathbf{p}}$ from Eqs. (49) and (50):

$$\frac{dn}{d^3\mathbf{p}'} \propto \exp\left(-\frac{1}{2m} p'_k (\mathbf{T}')^{-1}_{kl} p'_l\right), \quad k, l = x, y, z, \quad (56)$$

with summation understood over repeated indices. We introduced here the \mathbf{T}'_{kl} matrix and its inverse, \mathbf{T}'^{-1}_{kl} , as the matrix whose components correspond to the inverse slope parameters of the spectrum in the \overline{K}' frame. We find that the expression of these components is

$$T'_{xx} = T + m(\dot{X}^2 + \omega^2 R^2), \quad (57)$$

$$T'_{yy} = T + m\dot{Y}^2, \quad (58)$$

$$T'_{zz} = T + m(\dot{Z}^2 + \omega^2 R^2), \quad (59)$$

$$T'_{xz} = m\omega R(\dot{X} - \dot{Z}), \quad (60)$$

and for the inverse matrix:

$$\begin{pmatrix} T'_{xx} & T'_{xz} \\ T'_{xz} & T'_{zz} \end{pmatrix} \begin{pmatrix} T'^{-1}_{xx} & T'^{-1}_{xz} \\ T'^{-1}_{xz} & T'^{-1}_{zz} \end{pmatrix} = \begin{pmatrix} 1 & 0 \\ 0 & 1 \end{pmatrix}, \quad (61)$$

that is,

$$T'^{-1}_{xx} = \frac{T'_{zz}}{T'_{xx}T'_{zz} - T'^2_{xz}}, \quad (62)$$

$$T'^{-1}_{yy} = \frac{1}{T'_{yy}}, \quad (63)$$

$$T'^{-1}_{zz} = \frac{T'_{xx}}{T'_{xx}T'_{zz} - T'^2_{xz}}, \quad (64)$$

$$T'^{-1}_{xz} = \frac{-T'_{xz}}{T'_{xx}T'_{zz} - T'^2_{xz}}. \quad (65)$$

All time-dependent quantities: the axes X, Y, Z , their time derivatives, the R radius, the temperature T , and the „angular velocity“ ω from Eq. (37) are to be taken at the freeze-out time t_f , but for brevity we omit the

notation f in the index in these and in the following formulas.

We thus got a simple expression for the momentum distribution, much in the spirit of Ref. [15]. There it was emphasized that for a tilted, but not rotating ellipsoidal source, the momentum distribution is diagonal in exactly the same frame that corresponds to the tilted ellipsoid. We see that in our more realistic and general, rotating case, this is clearly not true: the presence of the cross-term in Eq. (56) signifies that the eigenframe of $N_1(\mathbf{p}')$ is not that of the coordinate-space ellipsoid, K' . We may introduce the angle $\vartheta'_{\mathbf{p}}$ that corresponds to the tilt of the eigenframe of the single particle spectrum with respect to the rotated ellipsoids, K' . This is given by

$$\tan(2\vartheta'_{\mathbf{p}}) = \frac{2T'_{xz}}{T'_{xx} - T'_{zz}} = \frac{2\omega R}{\dot{X} + \dot{Z}}. \quad (66)$$

Thus the observable tilt angle of the momentum spectrum, which we may denote by $\vartheta_{\mathbf{p}}$, becomes $\vartheta_{\mathbf{p}} \equiv \vartheta + \vartheta'_{\mathbf{p}}$. We see that the additional tilt $\vartheta'_{\mathbf{p}}$ of the momentum spectrum depends on how strong is the angular velocity ω that characterizes the rotation of the fireball geometry, as compared to an average radial Hubble flow, $\frac{\dot{X} + \dot{Z}}{2R}$. It is also maybe worthwhile to see that in our model, this $\vartheta'_{\mathbf{p}}$ angle does not depend on the particle mass m at all; as already hinted at, this gives an indication that in a Buda-Lund model type of relativistic extension (see the discussion before Section IV A) this angle will not depend on m_t .

We can also write up the momentum distribution in the original, laboratory frame (K) by the use of the matrix \mathbf{M} that connects \mathbf{p}' with \mathbf{p} in Eq. (53):

$$\frac{dn}{d^3\mathbf{p}} \propto \exp\left(-\frac{1}{2m}p_k(\mathbf{T})_{kl}^{-1}p_l\right), \quad k, l = x, y, z \quad (67)$$

where

$$\mathbf{T}^{-1} = \mathbf{M}^{-1}\mathbf{T}^{-1}\mathbf{M}. \quad (68)$$

Written up in components, the inverse slope parameters of the single-particle spectrum in the K frame are

$$T_{xx}^{-1} = T'^{-1}_{xx} \cos^2 \vartheta + T'^{-1}_{zz} \sin^2 \vartheta + T'^{-1}_{xz} \sin(2\vartheta), \quad (69)$$

$$T_{yy}^{-1} = T'^{-1}_{yy}, \quad (70)$$

$$T_{zz}^{-1} = T'^{-1}_{xx} \sin^2 \vartheta + T'^{-1}_{zz} \cos^2 \vartheta - T'^{-1}_{xz} \sin(2\vartheta), \quad (71)$$

$$T_{xz}^{-1} = T'^{-1}_{xz} \cos(2\vartheta) + (T'^{-1}_{zz} - T'^{-1}_{xx}) \cos \vartheta \sin \vartheta. \quad (72)$$

The difference to the formulas in Ref. [15] is again that the „intrinsic” cross-term, T'^{-1}_{xz} , does appear here: even in the $\vartheta_f = 0$ (hypothetical) case, one would get cross-terms in the single-particle spectrum. These non-vanishing cross-terms distinguish the truly rotating, tri-axial ellipsoidal fireballs from a tilted, three-dimensional expanding but non-rotating triaxial ellipsoid, discussed in Ref. [15].

C. Azimuthal anisotropies

We can also calculate the azimuthal dependence of the particle production, which is usually characterized by the v_n azimuthal harmonics. Remember, the z axis is taken as the axis of collision of the nuclei, and the x axis was taken to be the collision event plane, so the φ azimuthal angle is measured in the x - y plane. The definition of the azimuth-averaged single-particle spectrum $\frac{dn}{dp_t dy}$ and that of the v_n , $n = 1, 2, \dots$ anisotropy parameters is

$$\frac{dn}{d^3\mathbf{p}} = \frac{E}{2\pi p_t} \frac{dn}{dp_t dy} \left[1 + 2 \sum_{n=1}^{\infty} v_n \cos[n(\varphi - \Psi_n)] \right], \quad (73)$$

where $y = \frac{1}{2} \ln \frac{E+p_z}{E-p_z}$ is the rapidity, $p_t = \sqrt{p_x^2 + p_y^2}$ is the transverse momentum, and Ψ_n is called the n th order event plane angle.

The calculation of the v_n parameters and the angle-averaged spectrum in our case goes very much similarly if not identically to that found in Ref. [15]. There the case of a tilted but in itself not rotating ellipsoidal source was considered, and it was pointed out that the angle-averaged spectrum as well as the v_n parameters depend on the kinematical variables only through certain combinations of them. It is the case also here; the difference is that the expression of these scaling variables differ from the earlier results because of the presence of rotation in the velocity terms.

Introducing the w and v scaling variables and the average slope parameter T_{eff} as

$$T_{\text{eff}} \equiv \frac{2}{T_{xx}^{-1} + T_{yy}^{-1}}, \quad (74)$$

$$w \equiv \frac{p_t^2}{4m} (T_{xx}^{-1} - T_{yy}^{-1}), \quad v \equiv -\frac{p_t p_z}{m} T_{xz}^{-1}, \quad (75)$$

the single-particle spectrum can be written as

$$\frac{dn}{d^3\mathbf{p}} \propto \exp\left(-\frac{T_{zz}^{-1}}{2m}p_z^2 - \frac{p_t^2}{2mT_{\text{eff}}}\right) \times e^{w \cos(2\varphi) + v \cos \varphi}. \quad (76)$$

We can proceed from Eq. (76) by expanding the v -dependence in a series. Then using the $I_\nu(w) \equiv \frac{1}{\pi} \int_0^\pi d\varphi \cos(\nu\varphi) e^{w \cos \varphi}$ modified Bessel functions, we can do the Fourier decomposition in the φ dependence. It is important to note that in our simple model all the event planes coincide and this plane is where we set the zero of the azimuthal angle φ . We obtain the following:

$$\frac{dn}{2\pi p_t dp_t dy} \propto \exp\left(-\frac{T_{zz}^{-1}}{2m}p_z^2 - \frac{p_t^2}{2mT_{\text{eff}}}\right) \mathcal{I}_0(w, v), \quad (77)$$

$$v_n = \frac{\mathcal{I}_n(w, v)}{\mathcal{I}_0(w, v)}, \quad (78)$$

where the $\mathcal{I}_n(w, v)$ auxiliary quantities are expressed as

$$\mathcal{I}_{2p}(w, v) \equiv \sum_{k,l} \frac{I_{|k+p|}(w) + I_{|k-p|}(w)}{2^{2k+2l+1}(2k+l)!l!} v^{2k+2l}, \quad (79)$$

$$\mathcal{I}_{2p+1}(w, v) \equiv v \sum_{k,l} \frac{I_{|k+p|}(w) + I_{|k-p|}(w)}{2^{2k+2l}(2k+l)!(l+1)!} v^{2k+2l}. \quad (80)$$

In this latter formula, the summation over k and l formally goes over all integer values of them (including negative ones), but because of the factorials in the denominator, many terms will be zero.

We have given the full v -dependent expansion here. Practically, at mid-rapidity (ie around $p_z = 0$) only the first few terms in v are of interest. We give this here only for the first three anisotropy parameters, the v_1 (called directed flow), the v_2 (called the elliptic flow) and v_3 (which is sometimes called the third flow). The approximate expressions are:

$$\mathcal{I}_0(w, v) = I_0(w) + \frac{v^2}{4} [I_0(w) + I_1(w)] + \mathcal{O}(v^4), \quad (81)$$

$$v_1 = \frac{v}{2} \left[1 + \frac{I_1(w)}{I_0(w)} \right] + \mathcal{O}(v^3), \quad (82)$$

$$v_2 = \frac{I_1(w)}{I_0(w)} + \frac{v^2}{8} \left[1 + \frac{I_2(w)}{I_0(w)} - 2 \frac{I_1^2(w)}{I_0^2(w)} \right] + \mathcal{O}(v^4), \quad (83)$$

$$v_3 = \frac{v}{2} \frac{I_2(w) + I_1(w)}{I_0(w)} + \mathcal{O}(v^3). \quad (84)$$

The formulas obtained here are one-to-one copies of those found in Ref. [15]¹. The difference, as mentioned already, lies in the fact that the relation between the w, v scaling variables and the fundamental kinematical quantities is different here (because the \mathbf{T}^{-1} matrix contains the effect of rotation, not only the finite tilt angle). In particular, the apperarance of the non-zero cross term T'^{-1}_{xz} implies that T^{-1}_{xz} is nonzero even in the hypothetical case of zero ϑ_f tilt angle. Thus there is an interplay between the rotational motion of the fluid and the tilted state of the freeze-out ellipsoids that results in the characteristic rapidity and p_t dependence of the flow parameters through the w and v variables.

It is important to note that at mid-rapidity $p_z = 0$, hence $b = 0$, and we recover the simple universal scaling form of the elliptic flow, $v_2 = I_1(w)/I_0(w)$, so the triaxial, rotating and expanding ellipsoids have the same centrality, particle type, collision energy and transverse momentum independent universal scaling as predicted in Ref. [15], and extended to relativistic kinematics in Ref. [32]. In other words, triaxial ellipsoidal expansion does not spoil the universal scaling of the elliptic flow, but it modifies the definition of the scaling variable w .

D. Two-particle correlations

Using the formula Eq. (51) together with Eq. (49), a straightforward calculation leads to the following expression of the HBT correlation function in the K' frame (i.e. in the eigenframe of the tilted coordinate-space ellipsoid):

$$C(\mathbf{K}', \mathbf{q}') = 1 + \lambda \exp \left(- \sum_{k,l=x,y,z} q'_k \mathbf{R}'^2_{kl} q'_l \right). \quad (85)$$

Again, the exponent is easier to write down in this matrix form. The components of the \mathbf{R}'^2 matrix turn out to be

$$R'^2_{xx} = X^2 T T'^{-1}_{xx}, \quad (86)$$

$$R'^2_{yy} = Y^2 T T'^{-1}_{yy}, \quad (87)$$

$$R'^2_{zz} = Z^2 T T'^{-1}_{zz}, \quad (88)$$

$$R'^2_{xz} = X Z T T'^{-1}_{xz}, \quad (89)$$

where the components of the inverse temperature matrix \mathbf{T}'^{-1} are given by Eqs. (62)–(65).

The fact that the radius parameters do not depend on the total transverse momentum \mathbf{K} of the pair is a feature characteristic to the non-relativistic nature of the treatment and the self-similar nature of the solution [15]. Again, as before Section IV A, we mention that in a yet to be explored relativistic generalization, the HBT radii most probably depend on the transverse mass m_t of the pair approximately in the same way as they do depend on the particle mass m in the case of our exact non-relativistic solution. In our presented case this dependence is rather involved; it is given by Eqs. (86)–(89), which in turn refer to Eqs. (62) and (65) and Eqs. (57) and (60). However, it is not hard to see that a term with approximate $1/m$ -like dependence is present in the expression of the squared radius parameters, which implies the well-known and hydrodynamically predicted $1/R^2 = C_1 + C_2 \cdot m_t$ -like dependence of the R^2 components in the relativistic setting. In what follows, however, we again concentrate on the exact non-relativistic results, the relativistic generalization being outside of the scope of this paper.

To analyze the obtained HBT correlation further, we might again note that the final eigenframe of the rotating ellipsoid, K' is *not* the same as the frame in which the (Gaussian-like) HBT correlation function $C(\mathbf{q}')$ is diagonal. We denote the angle between K' and the eigenframe of the HBT correlation function by ϑ'_{HBT} . It turns out that this angle is not only non-zero, but in general different from ϑ'_p , the angle that described the eigenframe of the single-particle spectrum. The expression of ϑ'_{HBT} is

$$\begin{aligned} \tan(2\vartheta'_{\text{HBT}}) &= \frac{2XZT'_{xz}}{X^2T'_{zz} - Z^2T'_{xx}} = \\ &= \frac{2mXZ\omega R(\dot{X} - \dot{Z})}{(T + m\omega^2 R^2)(X^2 - Z^2) + m(X^2\dot{Z}^2 - Z^2\dot{X}^2)}, \end{aligned} \quad (90)$$

¹ We retained the notation v for the scaling variable introduced in Eq. (75) as a similar quantity appeared in Ref. [15]; it should not be confused neither with the flow quantities v_1, v_2, v_3, \dots , nor with the fluid velocity \mathbf{v} . Also, the w scaling variable should not be confused with the ω angular velocity parameter.

thus the observable tilt angle of the HBT correlation function, which we may denote by $\vartheta_{\mathbf{q}}$, becomes $\vartheta_{\mathbf{q}} \equiv \vartheta + \vartheta'_{\text{HBT}}$. In contrast to the $\vartheta'_{\mathbf{p}}$ angle introduced in Eq. (66), this ϑ'_{HBT} angle does depend on the mass of the particle, thus in a relativistic setting it may pick up an m_t -dependence. It might be interesting to note that by formally setting $m=0$ in the above formula, the ϑ'_{HBT} angle vanishes. Thus in the vanishing transverse mass limit the measurable tilt of the HBT system, $\vartheta_{\mathbf{q}}$ approaches the actual ϑ angle of tilt of the geometrical shape of the triaxial ellipsoid of the expanding and rotating fireball. The latter angle, denoted by ϑ up until now, may in this context thus be denoted by $\vartheta_{\mathbf{r}}$, being the geometrical tilt.

To write up the HBT correlation function in the laboratory frame (K frame), we only need to apply the matrix \mathbf{M} introduced in Eq. (19) to the components of \mathbf{q}' to express \mathbf{q}' with the components of the relative momentum measured in the K frame. Simple calculation leads to

$$C(\mathbf{K}, \mathbf{q}) = 1 + \lambda \exp \left(- \sum_{k,l=x,y,z} q_k \mathbf{R}_{kl}^2 q_l \right), \quad (91)$$

$$R_{xx}^2 = R_{xx}'^2 \cos^2 \vartheta + R_{zz}'^2 \sin^2 \vartheta + R_{xz}'^2 \sin(2\vartheta), \quad (92)$$

$$R_{yy}^2 = R_{yy}'^2, \quad (93)$$

$$R_{zz}^2 = R_{xx}'^2 \sin^2 \vartheta + R_{zz}'^2 \cos^2 \vartheta - R_{xz}'^2 \sin(2\vartheta), \quad (94)$$

$$R_{xz}^2 = R_{xz}'^2 \cos(2\vartheta) + (R_{zz}'^2 - R_{xx}'^2) \sin \vartheta \cos \vartheta. \quad (95)$$

We can also evaluate the HBT radius parameters suited for the usual setting of azimuthally sensitive HBT measurements, in the so-called Bertsch-Pratt (BP) or out-side-long frame. In this frame, the relative momentum vector \mathbf{q} is written up in the components (q_l, q_o, q_s) : the q_l („long”) component points in the beam (that is, the z) direction, the q_o („out”) component points to the direction of \mathbf{K} , the average transverse momentum of the pair, and q_s („side”) is the component perpendicular to both of these. We denote the azimuthal angle of \mathbf{K} in the x - y plane by φ , so

$$q_l = q_z, \quad (96)$$

$$q_o = q_x \cos \varphi + q_y \sin \varphi, \quad (97)$$

$$q_s = -q_x \sin \varphi + q_y \cos \varphi. \quad (98)$$

An important additional remark is in order here (just as in Ref. [15]): the preceding formulas were derived for instantaneous particle emission at time t_f . Assuming a finite Δt time duration of the particle emission (eg. by setting the time dependence as $(2\pi\Delta t^2)^{-1/2} \exp[-(t - t_f)^2/2\Delta t^2]$, a Gaussian) will have an effect on the HBT correlation function (although not on the single-particle spectrum). As in Refs. [15, 22], one gets the result that the radius parameters have to be augmented with an additional term $\delta R_{ij}^2 = \beta_i \beta_j \Delta t^2$, where $\beta = (\mathbf{p}_1 + \mathbf{p}_2)/(E_1 + E_2)$ is the velocity of the pair. In the Bertsch-Pratt frame $\beta_s = 0$, so finally we have the

correlation function as

$$C(\mathbf{K}', \mathbf{q}') = 1 + \lambda \exp \left(- \sum_{k,l=o,s,l} q_k \mathbf{R}_{kl}^2 q_l \right), \quad (99)$$

with the Bertsch-Pratt radius parameters being equal to

$$R_{oo}^2 = R_{xx}^2 \cos^2 \varphi + R_{yy}^2 \sin^2 \varphi + \beta_o^2 \Delta t^2, \quad (100)$$

$$R_{ss}^2 = R_{xx}^2 \sin^2 \varphi + R_{yy}^2 \cos^2 \varphi, \quad (101)$$

$$R_{ll}^2 = R_{zz}^2 + \beta_l^2 \Delta t^2, \quad (102)$$

$$R_{os}^2 = (R_{yy}^2 - R_{xx}^2) \sin \varphi \cos \varphi, \quad (103)$$

$$R_{ol}^2 = R_{xz}^2 \cos \varphi + \beta_l \beta_o \Delta t^2, \quad (104)$$

$$R_{sl}^2 = -R_{xz}^2 \sin \varphi. \quad (105)$$

Note that in the Longitudinally Co-Moving System, (LCMS), the above formulas simplify as in this system $\beta_l = 0$. In particular,

$$R_{ll}^2 = R_{zz}^2, \quad (106)$$

$$R_{ol}^2 = R_{xz}^2 \cos(\varphi), \quad (107)$$

hence in the LCMS we obtain the following interesting and experimentally easy and straightforward to test relation

$$R_{ol}^2(\varphi + \pi/2) = R_{sl}^2(\varphi), \quad (108)$$

and both terms oscillate in φ with half of the frequency of the oscillations of the side-side and out-out terms and the out-side cross-term.

The HBT correlation function is usually expressed in terms of the Bertsch-Pratt radii. We thus see how the oscillation of them (especially of the out-long, side-long components) is connected to the rotation of the flow. We also see evidently the emergence of a long-known fact that the φ -averaged $R_{oo}^2 - R_{ss}^2$ value (at a given m value) basically measures the life-time of the reaction: this is a frequently exploited feature, perhaps most recently in the already mentioned investigation of Ref. [17], where the non-monotonic behavior and finite-size scaling properties of this quantity is used to give a first indication on the presence of a critical endpoint on the phase diagram of QCD.

As an aside: note, however, that for expanding fire-shells with large temperature inhomogeneity and relatively small radial flows, typical for hadron-proton or proton-proton collisions, $R_{ss} < R_{oo}$ is also possible and actually expected at low transverse momentum, as predicted in Ref. [30] and as indicated as a robust feature of h+p and p+p reactions in Refs. [34–36].

V. ILLUSTRATION OF RESULTS AND DISCUSSION

We have demonstrated in the previous section how the rotating nature of the flow of our presented solution translates to the observable quantities. In this section we

illustrate the results obtained above by taking a reasonable set of initial conditions.

In the hydrodynamical equations we set the m_0 mass to be the proton mass, $m_0 = 938$ MeV, and start the time evolution with $T_0 = 300$ MeV. As an illustration, we take the initial conditions for the principal axes as $X_0 = 4$ fm, $Y_0 = 6$ fm, $Z_0 = 2$ fm, the initial ellipsoid being the thinnest in the beam direction, resembling the conditions right after a non-central heavy-ion collision. The ω_0 parameter is taken to be 0.15 c/fm. As said earlier, we make the assumption that the freeze-out happens instantaneously when the temperature reaches T_f , taken to be 140 MeV. (The parameter set employed here closely follows the one taken in Ref. [37] where the rotation effects in the spheroidal special case of our solution was studied.)

One of our goals in this section is to demonstrate that the final state observables carry information on the rotation and thus on the equation of state. In this work we do not investigate all the possible equations of state (including the $\mu_B = 0$ lattice QCD EoS, and those calculated for finite μ_B) in detail, we just want to give a hint at how the softness of the equation of state might influence the time development and the final state observables, deferring the detailed investigation to a follow-up work. Here we simply take different constant values of κ in the equation of state, Eq. (8). The conclusions that we arrive at with the initial conditions and assumptions should not thus be taken as general conclusions. But nevertheless, we will be able to draw some qualitative conclusions, and we will hint at which of the features of our results may carry over to a more general setting.

On Fig. 1 we plot the time development of the principal axes $X(t)$, $Y(t)$, $Z(t)$ of our solution for the mentioned initial conditions and parameters, for three different κ values. The higher the κ , the „softer” the equation of state is. On Fig. 2 we plot also the time development of the temperature $T(t)$ as well as that of the angular velocity $\omega(t)$. We denote the values of these quantities at the freeze-out by distinct markers.

Further, we plot the time development of the various tilt angles of the system introduced so far on Fig. 3. For this sake, we use the unified notation already introduced: $\vartheta_{\mathbf{r}} \equiv \vartheta$ denotes the tilt angle of the coordinate-space ellipsoids (eg. that of the level surfaces of the particle number density). However, as was pointed out, when rotation of the system plays a role, this angle is not accessible at first hand experimentally. Rather, what one can measure is the tilt angle corresponding to the eigenframe of the single-particle spectrum, which we can denote by $\vartheta_{\mathbf{p}} \equiv \vartheta + \vartheta'_{\mathbf{p}}$, where $\vartheta'_{\mathbf{p}}$ was introduced in Eq. (66), and measures the tilt of the eigenframe of the momentum spectrum with respect to the K' frame, which itself is tilted by $\vartheta_{\mathbf{r}} \equiv \vartheta$ in the laboratory frame. Another observable tilt angle is that of the eigenframe of the HBT correlation function, which we denote by $\vartheta_{\mathbf{q}} = \vartheta + \vartheta'_{\text{HBT}}$, where ϑ'_{HBT} measures the tilt angle of the HBT correlation function in the K' frame, and is introduced in

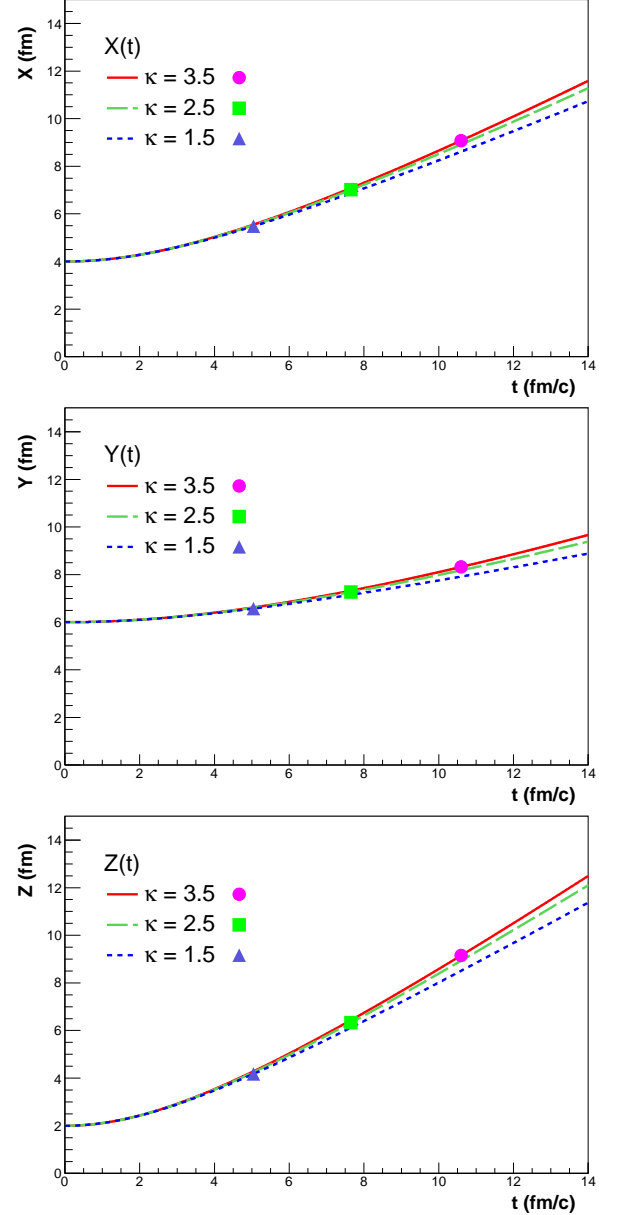


FIG. 1: Illustration of the dependence of the time evolution of principal axes $X(t)$, $Y(t)$, $Z(t)$ of the solution on the equation of state, for three different constant κ values. Initial conditions and parameters are: $m_0 = 938$ MeV, $T_0 = 300$ MeV, $\omega_0 = 0.15$ c/fm, $X_0 = 4$ fm, $Y_0 = 6$ fm, $Z_0 = 2$ fm, and $\dot{X}_0 = \dot{Y}_0 = \dot{Z}_0 = 0$. Markers denote the values at the respective freeze-outs (when the temperature reaches $T_f = 140$ MeV during time development).

Eq. (90). The initial value of these measured angles is sensitive to the precise initial conditions; e.g. the initial value of $\vartheta_{\mathbf{p}}$ of $\pi/4$ is due to the fact that our special initial conditions had $\dot{X}_0 = \dot{Y}_0 = \dot{Z}_0 = 0$. Nevertheless, one sees that by simultaneously measuring $\vartheta_{\mathbf{p}}$ and $\vartheta_{\mathbf{q}}$, one can infer the final rotation angle of the system, and one gets a quantity that is sensitive to the equation of state.

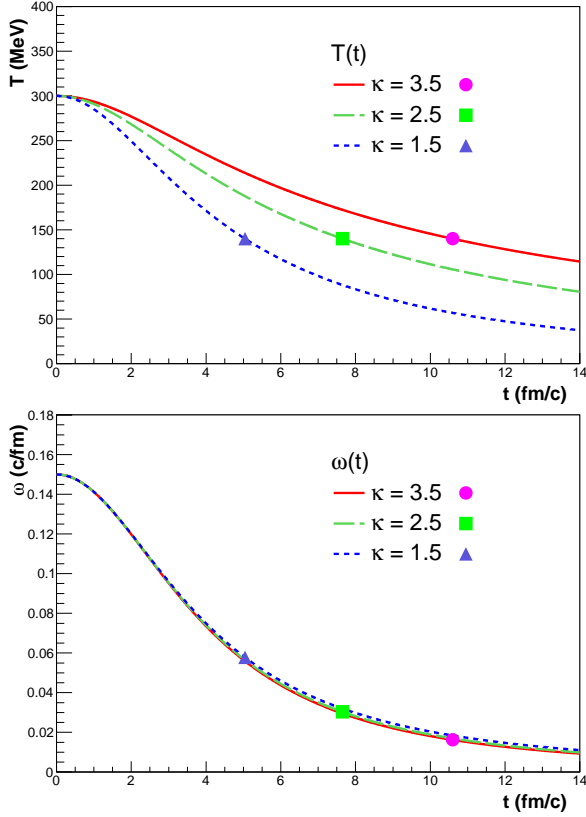


FIG. 2: Illustration of the dependence of the time evolution of the temperature $T(t)$ (upper panel) and the angular velocity $\omega(t)$ introduced in Eq. (37) on the equation of state, for three different constant κ values. Initial conditions and parameters are as in the previous example: $m_0 = 938$ MeV, $T_0 = 300$ MeV, $\omega_0 = 0.15$ c/fm, $X_0 = 4$ fm, $Y_0 = 6$ fm, $Z_0 = 2$ fm, and $\dot{X}_0 = \dot{Y}_0 = \dot{Z}_0 = 0$. Markers denote the values at the respective freeze-outs (when the temperature reaches $T_f = 140$ MeV).

We do not detail further investigations of more specific equation of states now. However, we note that in our plotted case, the EoS dependence of the final $\vartheta_{\mathbf{r}}$ tilt angle mainly comes from the fact that the adiabatic expansion lasts longer for a softer (i.e. that with a higher κ) equation of state. In the plotted case, i.e. when T_0 is kept fixed as κ changes, the change in the time development of the principal axes because of the change in κ has an opposite effect: we see from Figs. 1 and 2 that in this case, for softer κ the system expands *more* violently. In the plotted case the first effect dominates, so at the end of the day, softer κ will result in greater final tilt angle. It must be noted that if e.g. the total energy density is held fixed as κ changes, one can have a different conclusion, since in this case the time development will be *less* violent for softer κ . Since we do not have any a priori knowledge of the initial temperature or the initial energy density of the thermalized matter produced in various energy nucleus-nucleus collisions, in a realistic setting, the

conclusions evident on Figs. 1 and 2 may undergo significant changes. However, it is clear that besides the final (freeze-out) value of the $\omega(t)$ angular velocity, the final rotation angle of the system is a sensitive additional tool to investigate in the quest for the experimental equation of state of the strongly interacting matter.

Fig. 4 illustrates how the final, freeze-out tilt angles: the $\vartheta_{\mathbf{r}}$ (the coordinate-space tilt of the ellipsoid), and the two observable tilt angles, $\vartheta_{\mathbf{p}} \equiv \vartheta + \vartheta'_{\mathbf{p}}$ (the tilt of the single-particle spectrum), and $\vartheta_{\mathbf{q}} \equiv \vartheta + \vartheta'_{\text{HBT}}$ (the tilt of the HBT correlation function) depend on the initial condition ω_0 , and on the κ parameter in the EoS, respectively. All the other initial conditions and parameters in these plots are the same as those used for Fig. 3.

We plot some usual observable quantities such as the Bertsch-Pratt HBT radii given by Eqs. (100)–(105) as a function of pair azimuthal angle on Fig. 5, and the rapidity dependence of the azimuthal harmonics of the single particle spectrum, the v_1 directed flow, the v_2 elliptic flow, and the v_3 third flow on Fig. 6, for a reasonable set of parameter values at freeze-out. The intention of these plots is to illustrate the behavior of usual observables; we note that a combined measurement of all the HBT radii, including the R_{ol}^2 , R_{sl}^2 cross-terms is necessary to determine the ϑ'_{HBT} angle. In particular, as seen from Eqs. (100)–(105), the out-long and side-long cross-terms are the most characteristic to the tilted ellipsoidal source (as already pointed out in Refs. [14, 15]), but here we see that not only the final tilt angle but the rotational motion also gives a contribution to these parameters. Experimentally, the measurement of these cross-terms are the most daunting, because one has to have a combined event-by-event information on the first and second order event planes. In our simple hydrodynamical model, these event planes coincide, but in a realistic setting, both of them will be smeared by initial state fluctuations. Fig. 5 also illustrates the (108) relation between the R_{ol} and R_{sl} cross-terms: that in the LCMS, $R_{ol}^2(\phi + \pi/2) = R_{sl}^2(\phi)$, and both terms oscillate with half of the frequency of the oscillations of the other, more commonly measured out-out, side-side and out-side terms.

Also, a combined measurement of at least the slope of the $v_1(y)$, the p_t dependence of v_2 and the measurement of the angle-averaged single-particle spectrum is necessary to get the $\vartheta'_{\mathbf{p}}$ value. The most characteristic feature stemming from a tilted (or rotating) source in terms of the v_n parameters is perhaps the rapidity dependence of the v_1 directed flow; a feature already observed in experiment. However, in itself it is not enough to determine the tilt angle of the single-particle spectrum.

VI. SUMMARY AND OUTLOOK

We have presented a class of rotating expanding self-similar solutions of non-relativistic hydrodynamics that describe the expansion of a triaxial rotating ellipsoid, a realistic feature when applied to the rotating expansion

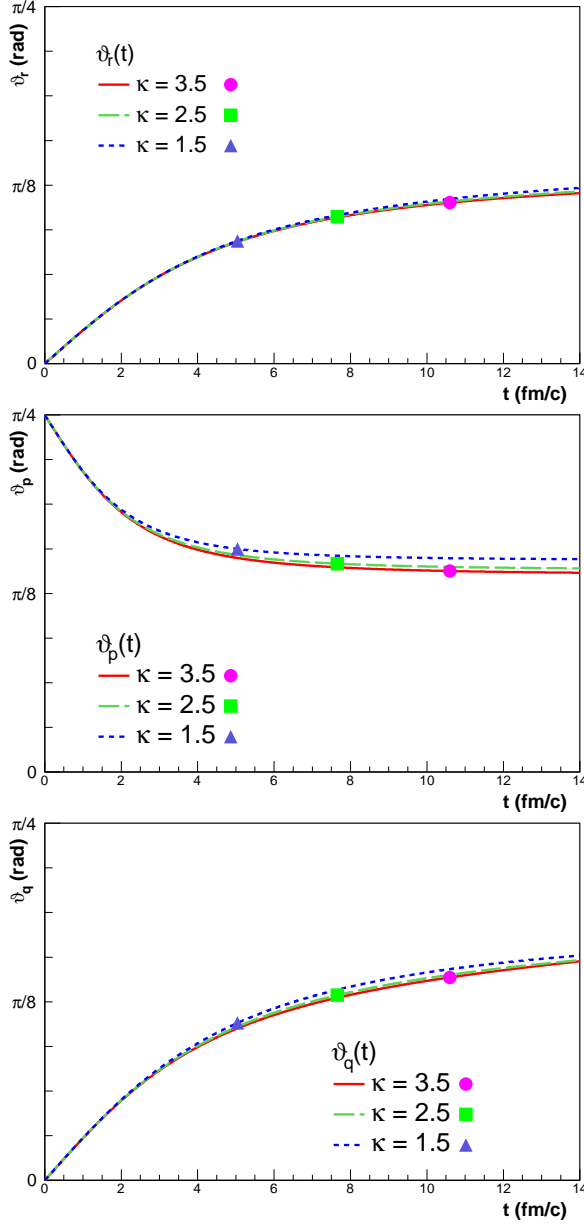


FIG. 3: Time development of the various tilt angles in our new hydrodynamical solution, for three different EoS. Parameters and initial conditions are the same as in Figs. 1 and 2, markers denote the values at the respective freeze-outs. Upper panel: the tilt angle of the coordinate-space ellipsoids in the x - z plane, ϑ_r , as introduced in the text. This is the tilt angle of the co-rotating K' frame. Middle panel: the ϑ_p angle, the observable tilt angle of the eigenframe of the single-particle spectrum ($\vartheta_p = \vartheta + \vartheta'_p$). Lower panel: ϑ_q , the tilt angle of the eigenframe of the HBT correlation function ($\vartheta_p = \vartheta + \vartheta'_{\text{HBT}}$). For plotting the ϑ_q angle, the mass of the pion m_π was used to evaluate ϑ'_{HBT} . As mentioned after Eq. (90), in the vanishing mass limit, $m \rightarrow 0$, this angle recovers the coordinate-space angle of tilt: $\vartheta_q \rightarrow \vartheta_r$.

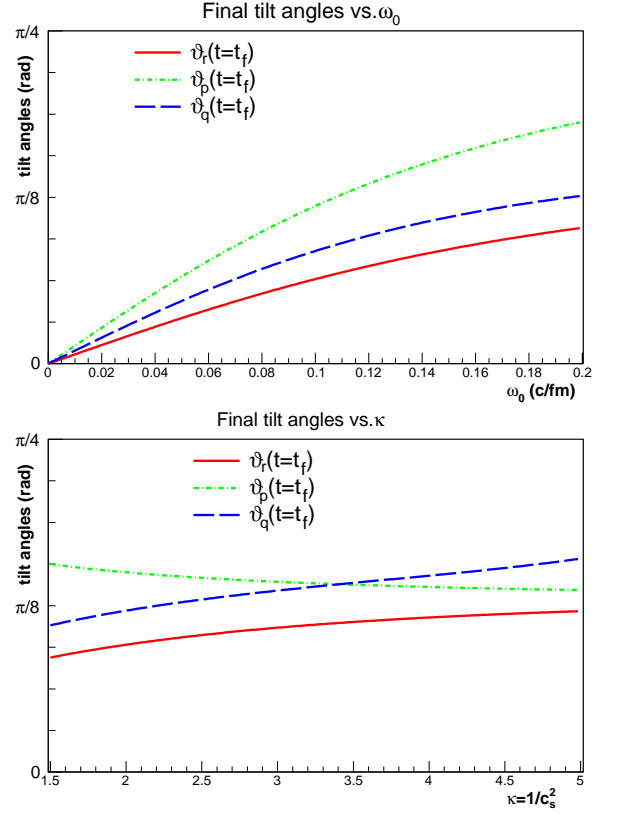


FIG. 4: The various tilt angles introduced in the text ($\vartheta_r \equiv \vartheta$, the coordinate-space tilt, $\vartheta_p \equiv \vartheta + \vartheta'_p$, the tilt of the single-particle spectrum, and $\vartheta_q \equiv \vartheta + \vartheta'_{\text{HBT}}$, the tilt of the HBT correlation function) at freeze-out time. Upper panel: freeze-out time angles plotted as a function of initial angular momentum ω_0 (for $\kappa = 3/2$). Lower panel: freeze-out time angles plotted as a function of κ (in this plot, the initial angular momentum was taken to be $\omega_0 = 0.15$ c/fm). All other initial conditions are the same as in Fig. 1.

of the matter produced in non-central heavy-ion collisions. The solution presented here can accommodate various equations of state, and is a natural generalization of earlier results describing rotating spheroids and non-rotating triaxial ellipsoids. We have evaluated single-particle spectra, flow (azimuthal anisotropy) parameters, two-particle Bose-Einstein correlations for this solution, using simple formulas that straightforwardly mirror the effect of rotation on the final state observables. The generality in the presented solution (that it allows for ellipsoids with three different principal axes) makes it possible to draw conclusions on the final state tilt angle, a quantity that in the case of spheroidal rotating solutions is either ill-defined or at least does not translate into the final state observables. This tilt angle is expected to behave non-monotonically around the softest point of the equation of state, which may correspond to the critical endpoint of QCD phase transitions.

Although in terms of observables we restricted our

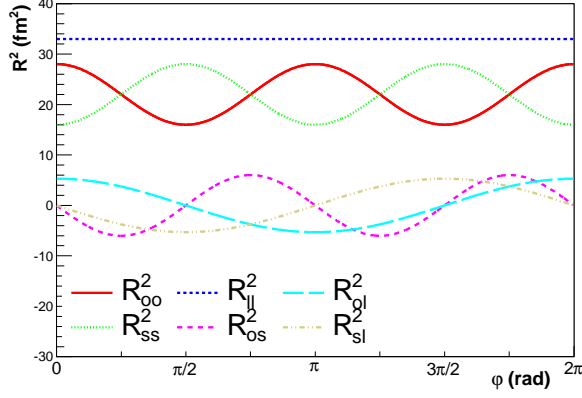


FIG. 5: Bertsch-Pratt HBT radii vs. ϕ azimuthal angle of the particle pair, calculated for a reasonable set of parameters: $R_{xx}^2 = 25 \text{ fm}^2$, $R_{yy}^2 = 16 \text{ fm}^2$, $R_{zz}^2 = 36 \text{ fm}^2$, $R_{xz}^2 = 2 \text{ fm}^2$, $\vartheta_f = \pi/8$. The oscillations in R_{oo}^2 , R_{ss}^2 and R_{os}^2 with π periodicity are characteristic to an ellipsoid-like source. The oscillations in R_{ol}^2 and R_{sl}^2 with 2π periodicity are characteristic to a tilted or rotating ellipsoid-like source. A measurement of these Bertsch-Pratt radii enables one to deduce the \mathbf{R} HBT radius matrix introduced in Eq. (91), and in turn the $\vartheta + \vartheta'_{\text{HBT}}$ angle introduced in Eq. (90), that characterizes the tilt of the eigenframe of the HBT correlation function. In this plot, the freeze-out is assumed to be instantaneous ($\Delta t = 0$), although in real data analysis Δt plays an important role.

selves to the exact non-relativistic solution discussed in the paper, we are confident that the general insight our treatment gives into the behavior of them will be useful in analyzing experimental data on single-particle spectra and HBT correlations. A relativistic generalization, although presently lacking as an actual hydrodynamical solution, maybe derived as a parametrization in the framework of the Buda-Lund hydrodynamical model. We made some preliminary remarks on this possibility throughout the paper.

We pointed out that in the general case of rotating *and* tilted source (on which our exact ellipsoidal hydrodynamical solution gives a fairly reasonable picture) the tilt angle of the ellipsoidal system is not identical to the tilt angle of the single-particle spectrum or that of the HBT correlation function. We derived expressions that connect these variables, and demonstrated their time dependence (and their values taken at the freeze-out of the hydrodynamical evolution) for a reasonable set of initial conditions, although a more detailed investigation of this dependence is beyond the scope of this paper.

In particular, we argued that the tilt angle observable from the oscillating HBT radii and from the single-particle spectrum becomes a non-monotonic function at the softest point of the equation of state, which suggest that this variable will be useful and straightforward to measure observable to signal the QCD critical point. We have also found that in the Longitudinal Center of Mass System of the boson pairs the out-long and the side-long

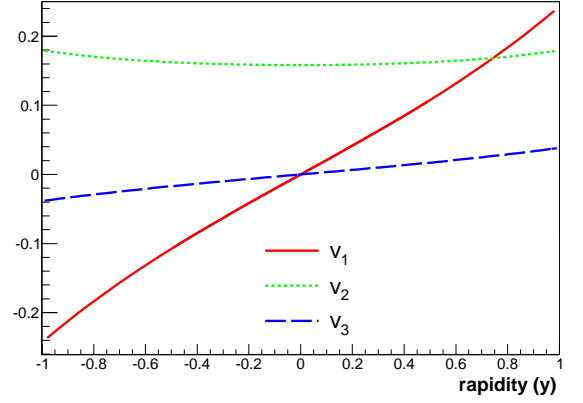


FIG. 6: Illustration of the dependence of flow parameters v_1 , v_2 , v_3 on rapidity y . The parameters were set to $T'_{xx} = 300 \text{ MeV}$, $T'_{xz} = -20 \text{ MeV}$, $T'_{zz} = 500 \text{ MeV}$, $T'_{yy} = 200 \text{ MeV}$, $\vartheta_f = \pi/8$. The p_t of the particles are assumed to be $p_t = 600 \text{ MeV}/c$, while the particle mass m was set to equal to the kaon mass, $m = 494 \text{ MeV}$. By measuring these flow coefficients and the angle-averaged spectrum, one can reconstruct the \mathbf{T} slope matrix elements introduced in Eq. (67), and in turn the angle ϑ'_p that characterizes the tilt of the eigenframe of the momentum distribution, as introduced in Eq. (66).

cross-terms oscillate for rotating and expanding triaxial hydrodynamical systems and they are phase-shifted by $\pi/2$ as compared to one another, providing straightforward experimental testing possibility for the qualitative features obeyed by in our new, rotating and expanding, triaxial ellipsoidal hydrodynamical solutions.

So the measurement of the rotation by means of the observables discussed in the paper might well give new insights into the equation of state of the quark-gluon plasma produced in high energy heavy-ion collisions, a main goal in today's heavy ion physics research. We thus look forward to the systematic experimental exploration of the rotation of the system produced in heavy ion collisions as a function of colliding beam energy, that might reveal a non-monotonic behavior of the equation of state as a function of temperature and baryochemical potential, and thus might help to locate and better characterize the deconfinement phase transition.

Acknowledgements

We would like to thank to M. Csanád, L. Csernai and Y. Hatta for inspiring discussions. The research of M. N. has been supported by the European Union and the State of Hungary, co-financed by the European Social Fund in the framework of TÁMOP 4.2.4. A/1-11-1-2012-0001 “National Excellence” Program, as well as by a Fulbright Research Grant for the 2015/2016 academic year. This work has been supported by the OTKA NK101438 grant of the Hungarian National Science Fund.

Appendix A: General linear rotating solution

In the body of the text, at the end of Section III B, we stated that the solution presented in the paper almost unequivocally follows from the ansatz that we made: that is, from the linearity of the velocity field, and the requirement that it describes self-similarly expanding ellipsoids in the K' frame that is rotated in the K frame around the y axis by angle $\vartheta(t)$. In this Appendix we elucidate this statement, and by doing so we write up the most general solution following from this ansatz. After exploring the general solution, we argue that the generality beyond that presented in the body of the paper is not relevant for the physical problem at hand.

The starting point is the (25) Euler equation in the K' frame, the (26) expression of the \mathbf{f}' inertial force density, the (29) expression of the velocity and the solutions (30) and (34) for the number density and the temperature. It turns out to be that in the case of non-homogeneous $T(\mathbf{r}', t)$, the condition (35) is necessary to arrive at a set of ordinary differential equations for the time-dependent quantities. (If Eq. (35) would not hold, it would be impossible to satisfy the Euler equation for all spatial coordinates with these velocity, temperature and density fields.) But if (35) holds, then the coordinate dependence of the Euler equation becomes simple: the x' component of the Euler equation will contain terms proportional to r'_x and terms proportional to r'_z , the y component only yields terms proportional to r'_y , and the z' components also contain terms proportional to r'_x and r'_z . For all of these to be satisfied for any \mathbf{r}' , we thus get five *ordinary* differential equations for $X(t)$, $Y(t)$, $Z(t)$, $\dot{\vartheta}(t)$ and $g(t)$. After some calculation, these turn out to be

$$-g^2 + \frac{\ddot{X}}{X} = \frac{T_0}{m_0} \left(\frac{V_0}{V} \right)^{\frac{1}{\kappa}} \frac{1}{X^2} + 2 \frac{Z}{X} g \dot{\vartheta} + \dot{\vartheta}^2, \quad (\text{A1})$$

$$\frac{\ddot{Y}}{Y} = \frac{T_0}{m_0} \left(\frac{V_0}{V} \right)^{\frac{1}{\kappa}} \frac{1}{Y^2}, \quad (\text{A2})$$

$$-g^2 + \frac{\ddot{Z}}{Z} = \frac{T_0}{m_0} \left(\frac{V_0}{V} \right)^{\frac{1}{\kappa}} \frac{1}{Z^2} + 2 \frac{X}{Z} g \dot{\vartheta} + \dot{\vartheta}^2, \quad (\text{A3})$$

$$\frac{X}{Z} \dot{g} + 2g \frac{\dot{X}}{Z} = -\ddot{\vartheta} - 2 \frac{\dot{Z}}{Z} \dot{\vartheta}, \quad (\text{A4})$$

$$\frac{Z}{X} \dot{g} + 2g \frac{\dot{Z}}{X} = -\ddot{\vartheta} - 2 \frac{\dot{X}}{X} \dot{\vartheta}. \quad (\text{A5})$$

If $X(t) \neq Z(t)$, then these last two equations can be cast into the form:

$$\frac{d}{dt} \left[(X+Z)^2 (g + \dot{\vartheta}) \right] = 0, \quad (\text{A6})$$

$$\frac{d}{dt} \left[(X-Z)^2 (g - \dot{\vartheta}) \right] = 0, \quad (\text{A7})$$

whose solutions are easily written up as

$$g(t) = \frac{\chi_0}{(X+Z)^2} + \frac{\xi_0}{(X-Z)^2}, \quad (\text{A8})$$

$$\dot{\vartheta}(t) = \frac{\chi_0}{(X+Z)^2} - \frac{\xi_0}{(X-Z)^2}, \quad (\text{A9})$$

with χ_0 and ξ_0 constants. Substituting these expressions back into Eqs. (A1)–(A3), we get

$$X \ddot{X} = \frac{T_0}{m_0} \left(\frac{V_0}{V} \right)^{\frac{1}{\kappa}} + \frac{2\chi_0^2 X}{(X+Z)^3} + \frac{2\xi_0^2 X}{(X-Z)^3}, \quad (\text{A10})$$

$$Y \ddot{Y} = \frac{T_0}{m_0} \left(\frac{V_0}{V} \right)^{\frac{1}{\kappa}}, \quad (\text{A11})$$

$$Z \ddot{Z} = \frac{T_0}{m_0} \left(\frac{V_0}{V} \right)^{\frac{1}{\kappa}} + \frac{2\chi_0^2 Z}{(X+Z)^3} - \frac{2\xi_0^2 Z}{(X-Z)^3}. \quad (\text{A12})$$

Now these equations for X , Y , Z can be written as the canonical equations from the following Hamiltonian:

$$H = \frac{1}{2m_0} (P_X^2 + P_Y^2 + P_Z^2) + U, \quad (\text{A13})$$

$$U = \kappa T_0 \left(\frac{V_0}{V} \right)^{1/\kappa} + \frac{m_0 \chi_0^2}{(X+Z)^2} + \frac{m_0 \xi_0^2}{(X-Z)^2}. \quad (\text{A14})$$

The most general solution of the hydrodynamical equations with the conditions stated at the beginning of this Appendix is thus given by the formulas for \mathbf{v}' , T and n , with the additional condition that the time development of $\dot{\vartheta}(t)$, $g(t)$ and the axes X , Y , Z follow Eqs. (A8)–(A9) and Eqs. (A10)–(A12).

We can calculate the conserved quantities for this general solution: the total particle number N_0 is again given by Eq. (43), the total energy turn out again to be equal to the Hamiltonian (A13), but the angular momentum J_z now contains a contribution determined by ξ_0 :

$$J_z = N_0 m_0 (\chi_0 - \xi_0). \quad (\text{A15})$$

The time development of the non-rotating ellipsoidal solution is fixed by six initial conditions: the initial values of the axes and their time derivatives. We are now investigating a rotating solution; we expect one additional free initial condition (that corresponds to e.g. the angular momentum of the flow). The appearance of the two new constants, χ_0 and ξ_0 in compare to the non-rotating case may thus seem superfluous. We have thus a justification to confine ourselves to the case when $\xi_0 = 0$, and in this case the additional initial condition, e.g. the value of J_z , is in one-to-one correspondence with the new constant, χ_0 . Also, as seen from the potential term (A14), in the case of $\xi_0 \neq 0$, there is an impenetrable potential barrier between the $X > Z$ and the $X < Z$ regions, so if the initial conditions satisfy $X_0 > Z_0$ (as it is physically plausible in the case of a heavy ion collision, see the discussion in Section V), then this relation will hold at any

future time. On the other hand, realistically one expects that during the time development, because of pressure gradients, eventually $X < Z$ will hold.

So we conclude that although the $\xi_0 \neq 0$ case might be interesting as some exotic rotating expanding flow, it is physically not what we are after in the quest for the description of a heavy-ion reaction. On the other hand, we can introduce new notation for the χ_0 constant, to conform with earlier results for rotating solutions:

$$\chi_0 \equiv 2\omega_0 R_0^2, \quad R_0 \equiv X_0 + Z_0, \quad (\text{A16})$$

with this we get the solution presented in Section III. Of course, for vanishing initial angular momentum we recover the earlier obtained directional Hubble flow profiles and ellipsoidal exact hydrodynamical solutions.

Returning to the 5 basic equations of motion, Eqs. (A1)–(A5), it is interesting to see what happens in the $X(t) = Z(t) \equiv R(t)$ case. In this case Eqs. (A1) and

(A3) are the same, so are Eqs. (A4) and (A5). So for the 4 quantities ($R, Y, \dot{\vartheta}, g$) there is only 3 equations:

$$R\ddot{R} = \frac{T_0}{m_0} \left(\frac{V_0}{V} \right)^{1/\kappa} + R^2 (g + \dot{\vartheta})^2, \quad (\text{A17})$$

$$Y\ddot{Y} = \frac{T_0}{m_0} \left(\frac{V_0}{V} \right)^{1/\kappa}, \quad (\text{A18})$$

$$\frac{d}{dt} [R^2 (g + \dot{\vartheta})] = 0. \quad (\text{A19})$$

So only the sum, $g + \dot{\vartheta}$ is uniquely determined: in the spheroidal case, one cannot unequivocally introduce the rotating K' frame and the angular velocity measured in that frame, only the total „angular velocity” of the fluid, which is $g + \dot{\vartheta}$. The remaining freedom in choosing g and $\dot{\vartheta}$ can be thought of as some kind of „gauge freedom”.

-
- [1] L. D. Landau, *Izv. Akad. Nauk Ser. Fiz.* **17**, 51 (1953).
 - [2] S. Z. Belenkij and L. D. Landau, *Nuovo Cim. Suppl.* **3S10**, 15 (1956) [*Usp. Fiz. Nauk* **56**, 309 (1955)].
 - [3] I.M. Khalatnikov, *Zhur. Eksp. Teor. Fiz.* **27**, 529 (1954).
 - [4] R. C. Hwa, *Phys. Rev. D* **10**, 2260 (1974).
 - [5] J. D. Bjorken, *Phys. Rev. D* **27**, 140 (1983).
 - [6] R. D. de Souza, T. Koide and T. Kodama, *arXiv:1506.03863 [nucl-th]*.
 - [7] L. P. Csernai, V. K. Magas, H. Stocker and D. D. Strottman, *Phys. Rev. C* **84**, 024914 (2011).
 - [8] L. P. Csernai, S. Velle and D. J. Wang, *Phys. Rev. C* **89**, no. 3, 034916 (2014).
 - [9] L. P. Csernai and S. Velle, *arXiv:1305.0385 [nucl-th]*.
 - [10] S. Velle, S. Mehrabi Pari and L. P. Csernai, *Phys. Lett. B* **757**, 501 (2016).
 - [11] F. Becattini, V. Chandra, L. Del Zanna and E. Grossi, *Annals Phys.* **338**, 32 (2013).
 - [12] F. Becattini, L. Csernai and D. J. Wang, *Phys. Rev. C* **88**, no. 3, 034905 (2013).
 - [13] Y. Xie, R. C. Glastad and L. P. Csernai, *arXiv:1505.07221 [nucl-th]*.
 - [14] M. A. Lisa, U. W. Heinz and U. A. Wiedemann, *Phys. Lett. B* **489**, 287 (2000).
 - [15] T. Csörgő, S. V. Akkelin, Y. Hama, B. Lukács and Y. M. Sinyukov, *Phys. Rev. C* **67**, 034904 (2003).
 - [16] R. A. Lacey, *Nucl. Phys. A* **931**, 904 (2014).
 - [17] R. A. Lacey, *Phys. Rev. Lett.* **114**, no. 14, 142301 (2015).
 - [18] Y. Hatta, J. Noronha and B. W. Xiao, *Phys. Rev. D* **89**, no. 5, 051702 (2014).
 - [19] Y. Hatta, J. Noronha and B. W. Xiao, *Phys. Rev. D* **89**, no. 11, 114011 (2014).
 - [20] M. I. Nagy, *Phys. Rev. C* **83**, 054901 (2011).
 - [21] T. Csörgő and M. I. Nagy, *Phys. Rev. C* **89**, no. 4, 044901 (2014).
 - [22] T. Csörgő, M. I. Nagy and I. F. Barna, *Phys. Rev. C* **93**, no. 2, 024916 (2016).
 - [23] J. P. Bondorf, S. I. A. Garpman and J. Zimanyi, *Nucl. Phys. A* **296**, 320 (1978).
 - [24] P. Csizmadia, T. Csörgő and B. Lukács, *Phys. Lett. B* **443**, 21 (1998).
 - [25] T. Csörgő, *Central Eur. J. Phys.* **2**, 556 (2004).
 - [26] T. Csörgő, *Acta Phys. Polon. B* **37**, 483 (2006).
 - [27] T. Csörgő, L. P. Csernai, Y. Hama and T. Kodama, *Heavy Ion Phys. A* **21**, 73 (2004).
 - [28] M. Csanád, M. I. Nagy and S. Lökös, *Eur. Phys. J. A* **48**, 173 (2012).
 - [29] M. Csanád and A. Szabó, *Phys. Rev. C* **90**, no. 5, 054911 (2014).
 - [30] T. Csörgő and B. Lörstad, *Phys. Rev. C* **54**, 1390 (1996).
 - [31] M. Csanád, T. Csörgő and B. Lörstad, *Nucl. Phys. A* **742**, 80 (2004).
 - [32] M. Csanád *et al.*, *Eur. Phys. J. A* **38**, 363 (2008).
 - [33] T. Csörgő, B. Lörstad and J. Zimányi, *Z. Phys. C* **71**, 491 (1996).
 - [34] N. M. Agababyan *et al.* [EHS/NA22 Collaboration], *Phys. Lett. B* **422**, 359 (1998).
 - [35] T. Csörgő, *Heavy Ion Phys.* **15**, 1 (2002).
 - [36] A. Bialas, W. Florkowski and K. Zalewski, *J. Phys. G* **42**, no. 4, 045001 (2015).
 - [37] L. P. Csernai, D. J. Wang and T. Csörgő, *Phys. Rev. C* **90**, no. 2, 024901 (2014).
 - [38] S. V. Akkelin, T. Csörgő, B. Lukács, Y. M. Sinyukov and M. Weiner, *Phys. Lett. B* **505**, 64 (2001).